Deuteron spin-spin relaxation study of second-order director fluctuations in the nematogen 5CB

Ronald Y. Dong
Department of Physics and Astronomy, Brandon University, Brandon, Manitoba, Canada R7A 6A9
and Physics Department, University of Manitoba, Winnipeg Manitoba, Canada R3T 2N2
(Received 2 September 1997; revised manuscript received 12 January 1998)

We report on a study of deuteron spin-spin relaxation times (T_2) at 46 MHz in the perdeuterated liquid crystal 4-*n*-pentyl-cyanobiphenyl (5CB). By combining with previously measured deuteron spin-lattice relaxation rates, we have derived the spectral densities of motion $J_0(0)$,$J_1(\omega_0)$, and $J_2(2\omega_0)$ for various carbon sites of 5CB. In our global target analysis of all the spectral density data, a model that relies on molecular reorientations, internal rotations in the flexible chain, and director fluctuations as relaxation mechanisms is used. We found that director fluctuations make an insignificant contribution to $J_1(\omega_0)$ because 5CB has a high cutoff frequency smaller than our Larmor frequencies, but make a nonzero contribution to $J_0(0)$. According to the theory, director fluctuations can only affect $J_0(0)$ via a second-order contribution. Our T_2 data seem to be consistent with the prediction of the director fluctuation theory. Model parameters that include rotational diffusion constants, internal jump constants, and the prefactor A of director fluctuations have been determined as a function of temperature. [S1063-651X(98)13204-X]

PACS number(s): 61.30.−v

I. INTRODUCTION

It is well known that director fluctuations [1–3] can be an important source of nuclear spin relaxation in liquid crystals. Deuterium nuclear magnetic resonance (NMR) has been used to examine both solvent and solute spins in liquid crystals [4]. The detection of director fluctuations of solvent spins by deuteron spin-lattice relaxation measurements at conventional NMR frequencies has met [5–7] with limited success. Indeed, NMR field-cycling techniques [8] are useful in studying director fluctuations in the kilohertz region. However, we have recently demonstrated [9] that the deuteron spin-spin relaxation time (T_2) measurement in a liquid crystal can detect higher-order director fluctuations at a standard high field. The liquid crystal 4-*n*-pentyl-cyanobiphenyl (5CB) has been studied using NMR by several research groups [10–13] and is chosen in the present study since its deuteron spin-lattice relaxation rates measured in the MHz region have been found [11] to be unaffected by director fluctuations. In this paper, we use a model that includes second-order director fluctuations, molecular reorientations, and internal bond rotations, to quantitatively explain the T_2 data of 5CB.

The director fluctuation mode spectrum depends on many factors such as the viscoelastic constants of the medium, molecular length, domain size, temperature, and the degree of ordering in the sample. In the small angle (θ) approximation, director fluctuations contribute [1] a frequency term to the spectral density $J_1(\omega)$, and have zero contributions to $J_0(\omega)$ and $J_2(2\omega)$. Since director fluctuations must involve collective motions of many molecules, the mode spectrum has a high cutoff frequency [14] that depends on sample properties. To explain the observed frequency dependence in J_2 for strongly ordered solutes in liquid crystals, second-order director fluctuations ($\propto \theta^2$) have been considered [15–17]. The calculated frequency dependence in J_2 was generally too small. Recently Joghems and van der Zwan [18] argued that there is an overestimation of director fluctuations in $J_1(\omega)$ unless one also includes second-order director fluctuations. Therefore, director fluctuations make contributions to all spectral densities when the small angle approximation is removed. When the high cutoff frequency is of the order of a few MHz, director fluctuations become ineffective for spin relaxation in the MHz regime. In the present study, we show that 5CB has a high cutoff frequency of the order of 1 MHz. At our Larmor frequencies, the complication of a small cross term [19,20] between molecular motions and director fluctuations will be ignored.

Besides director fluctuations, molecular motions and internal bond rotations also play a role in relaxing the deuteron spin. Here Nordio's model [21] is used to describe the molecular reorientation and a decoupled model [22] to describe correlated internal rotations in the flexible chain of 5CB. Both these models have been used to interpret the spin-lattice relaxation times T_{1Z} and T_{1Q} of several liquid crystals including 5CB [11]. A global target approach [23] has recently been applied to analyze the spin relaxation data [24] of a liquid crystal. By analyzing the data at all temperatures and different frequencies, one can obtain more reliable target model parameters. In the present work, we adopt the same approach to analyze both the spin-spin and spin-lattice relaxation data of 5CB. The paper is organized as follows. In Sec. II, the experimental method is given. The basic theory needed to interpret the experiments is given in Sec. III. The last section contains results and discussion.

II. EXPERIMENTAL METHOD

The nematic liquid crystal 4-*n*-pentyl-d_{11}-4′-cyanobiphenyl-d_4 (5CB-d_{15}) is the one used in our previous T_1 study [11]. The sample has a clearing temperature (T_c) of 35.3 °C. A home-built superheterodyne coherent pulse NMR spectrometer was operated for deuterons at the Larmor frequency of 46 MHz using an Oxford 7 T superconducting magnet. The sample director was aligned along the magnetic field. A quadrupolar echo pulse train [25],

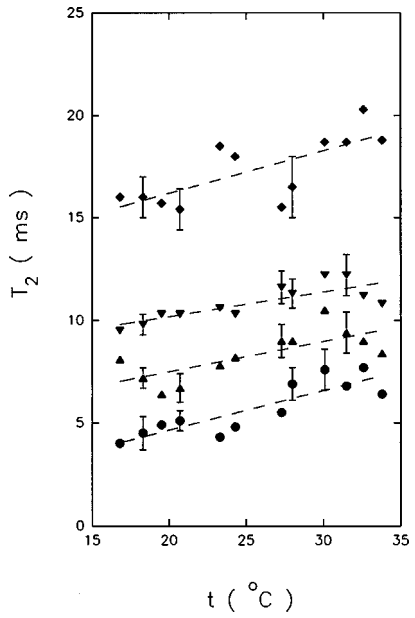

FIG. 1. Experimental spin-spin relaxation times vs the temperature in the nematic phase of 5CB. The circles, upward triangles, downward triangles and diamonds denote data from C_1, C_2, C_3, and C_4, respectively. The dashed lines are drawn to aid the eye.

90_x-τ-90_y-$(2\tau$-$90_y)_n$-, with an eight-step phase cycling scheme was used to measure T_2. Typical 90° pulse length was about 4 μs. Pulse control and signal collection were done using a General Electric 1280 minicomputer. Free induction decays (FIDs) after the last 90° pulse for different n were recorded with quadrature detection and then fast Fourier transformed to obtain deuterium spectra. At 46 MHz, FID signals were averaged over 8 scans with a repetition time 400 ms or longer. The sample temperature in the NMR probe was regulated by an air flow with a Bruker BST-1000 temperature controller. Sample heating due to multiple pulse sequences was minimal ($<0.5°$). Each T_2 experiment consisted of 32 different n (e.g., $n=1,3,6,9,\ldots,96$) values. A plot of the peak intensity of a quadrupolar doublet versus $2n\tau$ was used to determine T_2. Ahmad *et al.* [26] have shown that the measured T_2 depended on the pulse spacing τ. Two limiting cases could be considered. When the pulse spacing $\tau \ll 1/\nu_Q$ with $2\nu_Q=\Delta\nu$ being the quadrupolar splitting of the deuteron in question, the deuteron spin relaxed as if the splitting was absent. This limit was not feasible experimentally because of rather large quadrupolar splittings in liquid crystals and overheating of the sample by the rf pulse train. At the other limit ($\tau > 1/\nu_Q$), the two lines of the doublet relaxed independently to give the spin-spin relaxation rate $R_2=(T_2)^{-1}$:

$$R_2=\tfrac{3}{2}J_0(0)+\tfrac{3}{2}J_1(\omega_0)+J_2(2\omega_0), \tag{1}$$

where $\omega_0/2\pi$ is the Larmor frequency. Due to the smaller quadrupolar splittings of the methyl and ring deuterons, we only measured T_2 for the methylene deuterons of the pentyl chain. The pulse spacing τ was set at 160 μs to satisfy the $\tau > 1/\nu_Q$ condition for all the deuterons under study (to include ring deuterons would need a large τ, and cause drops in echo intensities). These T_2 values are shown as a function of temperature in Fig. 1. The errors in our T_2 measurements were estimated to be $\pm$ 10%. To determine $J_0(0)$ from Eq. (1), previously measured J_1 and J_2 values at 46 MHz [11] were used. It is noted that previous T_{1Z} and T_{1Q} could be reproduced within experimental errors in the same sample and the temperatures of the sample for the T_1 and T_2 measurements were calibrated using the quadrupolar splittings as an internal standard. Because of experimental uncertainties in J_1, J_2, and T_2 values, the derived $J_0(0)$ values tend to have larger errors.

III. THEORY

We first outline the spin relaxation theory [1,2] of director fluctuations. When fluctuations in the orientation of director include terms up to second order ($\propto\theta^2$), all spectral densities $J_0(0)$, $J_1(\omega_0)$, and $J_2(2\omega_0)$ have nonzero contributions [15–18]. For the ith deuterons, which reside on the rigid part of a molecule (assume uniaxial when treating director fluctuations), the spectral densities J_0 and J_2 are given by [16]

$$J^{(i)}_{2\mathrm{DF}}(\omega)=J^{(i)}_{0\mathrm{DF}}(\omega)/3=\frac{1}{3\pi}K_Q^{(i)}A^2S_0^2[d^2_{00}(\beta^{(i)}_{M,Q})]^2 \times\ln[1+(\omega_c/\omega)^2], \tag{2}$$

where $K_Q=(3\pi^2/2)(q_{\mathrm{CD}})^2$ with q_{CD} being the quadrupolar coupling constant (e^2qQ/h), and $\beta_{M,Q}$ is the angle between the C—D bond and the molecular z_M axis. The high cutoff frequency ω_c is given in terms of the cutoff wave vector q_c by $\omega_c=Kq_c^2/\eta$ where K is the average elastic constant and η the average viscosity. S_0 is the nematic order parameter of the molecule relative to the local director, and is related to the usual nematic order parameter $\langle P_2\rangle$ according to [27]

$$S_0=\langle P_2\rangle/(1-3\alpha), \tag{3}$$

where the parameter $\alpha=kTq_c/2\pi^2K$ is a measure of the magnitude of director fluctuations. A typical α value derived from deuteron NMR studies is $\sim$0.04 for MBBA (p-methoxybenzylidene-p-n-butylaniline) and $\sim$0.1 for 4O.8 [28]. A is the standard prefactor [2] for director fluctuations

$$A=\frac{3kT}{4\sqrt{2}\pi}(\eta/K^3)^{1/2}=3\pi\alpha/\sqrt{8\omega_c}. \tag{4}$$

Now Eq. (2) gives a $J^{(i)}_{0\mathrm{DF}}(\omega)$ expression, which unfortunately diverges as $\omega\to0$. To remove the divergence, a low cutoff frequency is required [19]. However, this does not give an analytical expression. A less exact procedure is used [16] to obtain the following expression for the limit $\omega\to0$:

$$J^{(i)}_{0\mathrm{DF}}(\omega)=K_Q^{(i)}A^2S_0^2[d^2_{00}(\beta^{(i)}_{M,Q})]^2\frac{1}{\pi}\ln\left(\frac{1+(\omega_c/\omega)^2}{1+(\omega_1/\omega)^2}\right), \tag{5}$$

where the frequency ω_1 may be estimated in the presence of the magnetic field, i.e., $\omega_1=K/\eta\xi^2$ and the magnetic coherence length $\xi=(\mu_0K/\Delta\chi B^2)^{1/2}$ with $\Delta\chi$ being the anisotropic part of the molecular diamagnetic susceptibility. Now the spectral density $J_1(\omega)$ due to director fluctuations is given by [18]

$$J^{(i)}_{1\mathrm{DF}}(\omega)=K^{(i)}_{Q}AS^{2}_{0}[d^{2}_{00}(\beta^{(i)}_{M,Q})]^{2}(1-4\alpha)U(\omega_{c}/\omega)/\omega^{1/2}, \tag{6}$$

where the cutoff function [19] $U(x)$,

$$U(x)=\frac{1}{2\pi}\ln\left[\frac{x-\sqrt{2x}+1}{x+\sqrt{2x}+1}\right]+\frac{1}{\pi}[\tan^{-1}(\sqrt{2x}-1)+\tan^{-1}(\sqrt{2x}+1)], \tag{7}$$

is to limit coherent modes in the director fluctuation spectrum by a high cutoff frequency. The factor $(1-4\alpha)$ is needed when second-order director fluctuations are taken in account. For 5CB, $U(x)$ is close to zero at our Larmor frequencies (46 and 15.3 MHz) when a high cutoff frequency of 1 MHz is used.

For C—D bonds located in a flexible chain, the effect of director fluctuations is made smaller due to additional averaging by rapid conformational changes within the chain. Thus the geometric factor in Eqs. (2), (5), and (6) must involve an additional conformational average and together with $\langle P_2\rangle$ can be replaced [5,28] by the segmental order parameter S_{CD} (or in terms of the quadrupolar splitting) of the ith deuterons. Thus, director fluctuations contribute to the chain deuterons according to

$$J^{(i)}_{0\mathrm{DF}}(\omega)=\frac{3\pi^{2}}{2}(q^{(i)}_{\mathrm{CD}})^{2}\frac{A^{2}}{(1-3\alpha)^{2}}(S^{(i)}_{\mathrm{CD}})^{2}\frac{1}{\pi}\ln\left[\frac{1+(\omega_{c}/\omega)^{2}}{1+(\omega_{1}/\omega)^{2}}\right], \tag{8}$$

$$J^{(i)}_{1\mathrm{DF}}(\omega)=\frac{3\pi^{2}}{2}(q^{(i)}_{\mathrm{CD}})^{2}\frac{A}{(1-3\alpha)^{2}}(S^{(i)}_{\mathrm{CD}})^{2}\times(1-4\alpha)U(\omega_{c}/\omega)/\sqrt{\omega}, \tag{9}$$

$$J^{(i)}_{2\mathrm{DF}}(2\omega)=\frac{3\pi^{2}}{2}(q^{(i)}_{\mathrm{CD}})^{2}\frac{A^{2}}{(1-3\alpha)^{2}}(S^{(i)}_{\mathrm{CD}})^{2}\frac{1}{3\pi}\times\ln[1+(\omega_{c}/2\omega)^{2}]. \tag{10}$$

It is noted that in all these equations, the contributions from director fluctuations to J_0, J_1, and J_2 are all related to the high cutoff frequency ω_c. For the molecule 5CB, only Eq. (8) is relevant in our calculations. To minimize the total number of model parameters in fitting the spectral density data, only the prefactor A (or α) is used as an adjustable parameter to determine the strength of director fluctuations in the present study.

To describe the reorientation of an asymmetric molecule in an uniaxial medium, one must find the conditional probability for the molecule to take a certain orientation given at time zero it has a different orientation. This is done by solving a rotational diffusion equation. The symmetrized rotational diffusion operator [29] $\hat{\Gamma}$ is given in terms of an asymmetry parameter of the rotational diffusion tensor $\epsilon=(D_x-D_y)/(D_x+D_y)$, and $\eta=D_z/\rho$ where $\rho=(D_x+D_y)/2$; D_x, D_y and D_z are the principal elements of a rotational diffusion tensor, defined in a molecular frame fixed on the molecule. In the case of flexible molecules, the rotational diffusion tensor refers to the motion of an ''average'' conformer whose ϵ is set to zero in the present study. In other words, the 81 different conformations (we allow the first dihedral angle in the pentyl chain to sample all three rotameric states) of 5CB are assumed to share the same rotational diffusion constants and the ''average'' conformer to have a uniaxial diffusion tensor [21]. The molecular frame is taken [11] with its molecular z_M along the ring para axes. In general, the orientational correlation functions can be written as a sum of decaying exponentials [21,29]:

$$G^{2}_{mnn'}(t)=\sum_{K}(\beta^{2}_{mnn'})_{K}\exp[(\alpha^{2}_{mnn'})_{K}t], \tag{11}$$

where m and $n(n')$ represent the projection indices of a rank 2 tensor in the laboratory and molecular frames, respectively; $(\alpha^{2}_{mnn'})_K/\rho$, the decay constants, are the eigenvalues of the $\hat{\Gamma}$ matrix and $(\beta^{2}_{mnn'})_K$, the relative weights of the exponentials, are the corresponding eigenvectors.

The spectral densities for a deuteron residing on the rigid part of a uniaxial molecule ($n=n'$) are the Fourier transform of the time correlation functions ($m=0,1$, or 2) to give

$$J_{mR}(m\omega)=\frac{3\pi^{2}}{2}(q_{\mathrm{CD}})^{2}\sum_{n}[d^{2}_{n,0}(\beta_{M,Q})]^{2}\times\sum_{K}\frac{(\beta^{2}_{mnn})^{2}_{K}(\alpha^{2}_{mnn})^{2}_{K}}{(\alpha^{2}_{mnn})^{2}_{K}+m^{2}\omega^{2}}, \tag{12}$$

where the subscript R is used to denote the molecular rotation. For the ring deuterons, the above equation must be modified to include internal ring rotations [30] (with a rotational diffusion constant D_R) about its para axis and q_{CD} = 185 kHz. The ring rotation is treated in the strong collision limit. For the deuterons in the chain, a decoupled model [22] is used to describe correlated internal rotations in the flexible pentyl chain. The spectral densities can be written as [2]

$$J^{(i)}_{mR}(m\omega)=\frac{3\pi^{2}}{2}(q^{(i)}_{\mathrm{CD}})^{2}\sum_{n}\sum_{k=1}^{81}\left|\sum_{l=1}^{81}d^{2}_{n,0}(\beta^{(i)l}_{M,Q})\exp[-in\alpha^{(i)l}_{M,Q}]x^{(1)}_{l}x^{(k)}_{l}\right|^{2}\sum_{K}\frac{(\beta^{2}_{mnn})_{K}[(\alpha^{2}_{mnn})_{K}+|\lambda_{k}|]}{[(\alpha^{2}_{mnn})_{K}+|\lambda_{k}|]^{2}+m^{2}\omega^{2}}$$
$$+\frac{3\pi^{2}}{2}(q^{(i)}_{\mathrm{CD}})^{2}\delta_{m0}\langle P_2\rangle^{2}\sum_{k=1}^{81}\left|\sum_{l=1}^{81}d^{2}_{00}(\beta^{(i)l}_{M,Q})x^{(1)}_{l}x^{(k)}_{l}\right|^{2}\Big/|\lambda_{k}|, \tag{13}$$

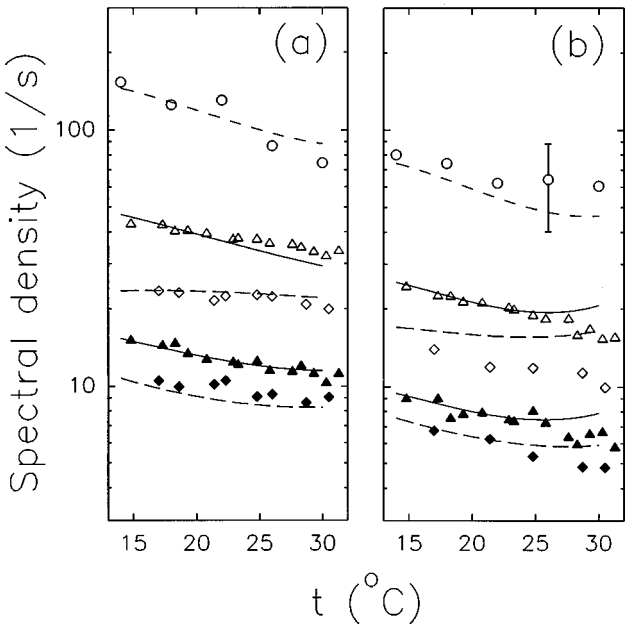

FIG. 2. Experimental (symbols) and fitted (lines) spectral densities of 5CB-d_{15}. (a) and (b) are for C_1, and C_2, respectively. The open circles denote the spectral densities $J_0(0)$, the open triangles and diamonds denote $J_1(\omega_0)$, while the closed triangles and diamonds denote $J_2(2\omega_0)$. The triangles represent the data at 15.3 MHz, while the diamonds represent data at 46 MHz. Solid and long dashed lines denote fitted spectral densities at 15.3 and 46 MHz, respectively. Both J_1 and J_2 data were reproduced from Ref. [11].

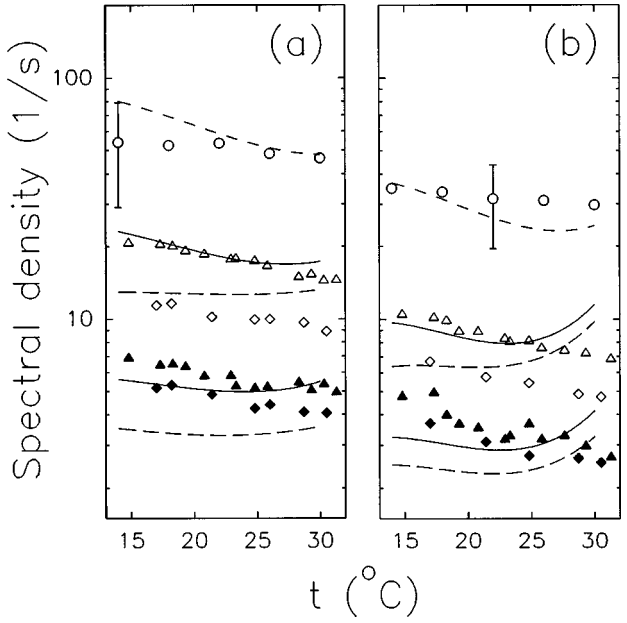

FIG. 3. Experimental (symbols) and fitted (lines) spectral densities of 5CB-d_{15}. (a), and (b) are for C_3, and C_4, respectively. The legends are the same as those in Fig. 2.

where $q_{\mathrm{CD}}^{(i)} = 165$ kHz, $\beta_{M,Q}^{(i)l}$ and $\alpha_{M,Q}^{(i)l}$ are the polar angles of the C_i—D bond of the conformer l in the molecular frame, λ_k and $\vec{x}^{(k)}$ are the eigenvalues and eigenvectors from diagonalizing a symmetrized transition rate matrix. The rate matrix describing conformational changes in the pentyl chain has the dimension of 81×81, and contains jump constants k_1, k_2, and k_3 for one-, two- and three-bond motions [22] in the chain. Finally, the spectral densities for the ith deuterons are calculated from

$$J_1^{(i)}(\omega) = J_{1R}^{(i)}(\omega), \tag{14}$$

$$J_2^{(i)}(2\omega) = J_{2R}^{(i)}(2\omega), \tag{15}$$

$$J_0^{(i)}(0) = J_{0R}^{(i)}(0) + J_{0\mathrm{DF}}^{(i)}(0), \tag{16}$$

where $i = 0$, 1, 2, 3, and 4 with $i = 0$ denoting the ring site. It is noted that for 5CB, director fluctuations do not contribute to J_1 and J_2 in Eqs. (14) and (15). Using Eqs. (8), (12), and (13) in the above equations, the 7 model parameters (D_x, D_z, D_R, k_1, k_2, k_3, and A) can be varied to fit the 24 experimental spectral densities at each temperature.

IV. RESULTS AND DISCUSSION

The spectral densities $J_1^{(i)}(\omega_0)$ and $J_2^{(i)}(2\omega_0)$ for the chain carbon (i = 1–5) and ring ($i = 0$) deuterons at 15.3 and 46 MHz are reproduced [11] in Figs. 2–4. Since the T_2 measurements are limited in the temperature range and those obtained close to the T_c appear to be particularly sensitive to experimental errors, only spectral densities from the T_1 data between 14° and 32 °C are reproduced here. The $J_0^{(i)}(0)$ for the methylene deuterons (i = 1–4) are derived from Eq. (1) and shown also in Figs. 2 and 3. The earlier analysis of quadrupolar splittings [11] using internal energies $E_{tg} = 3.8$ kJ/mol and $E_{gg} = 0$ kJ/mol gave the potential of mean torque ($X_a, \lambda_c = X_c/X_a$) and order parameters ($\langle P_2 \rangle$ and $S_{xx} - S_{yy}$) used in our current analysis. As noted before the average conformer of 5CB is essentially uniaxial because of its small $S_{xx} - S_{yy}$ values (~ 0.006). However, the order parameter tensor allows us to adopt a biaxial orienting potential (specified by a_{20}, a_{22}) for solving the rotational diffusion equation in the manner described by Tarroni and Zannoni [29] [despite the fact that $n = n'$ was used in Eqs. (12) and (13)]. To increase the number of measured spectral densities in our fitting procedure, we have chosen to simultaneously treat the spectral density (J_1 and J_2 of ring C_0 and methylene C_i (i=1–4) deuterons, and J_0 of the methylene deuterons) data at five different temperatures in the nematic phase of 5CB. We do not consider the methyl group because of the complication from its fast threefold rotation [31]. This so-called global target analysis takes advantage of the fact that target parameters of the model vary smoothly with temperature. The method, however, requires assuming (or knowing) the temperature dependences of the model parameters. Therefore, individual target analysis (i.e., fitting experimental spectral densities at a single temperature) must first be performed to get an idea on the temperature relations of these model parameters. Smoothed lines of data were used to obtain the $J_0^{(i)\mathrm{expt}}(0)$, $J_1^{(i)\mathrm{expt}}(\omega_0)$ and $J_2^{(i)\mathrm{expt}}(2\omega_0)$ values at the chosen temperatures. An optimization routine [32] (AMOEBA) is used to minimize the sum squared error F,

$$F = \sum_k \sum_{\omega_0} \sum_i \sum_m [J_m^{(i)\mathrm{calc}}(m\omega_0) - J_m^{(i)\mathrm{expt}}(m\omega_0)]_k^2, \tag{17}$$

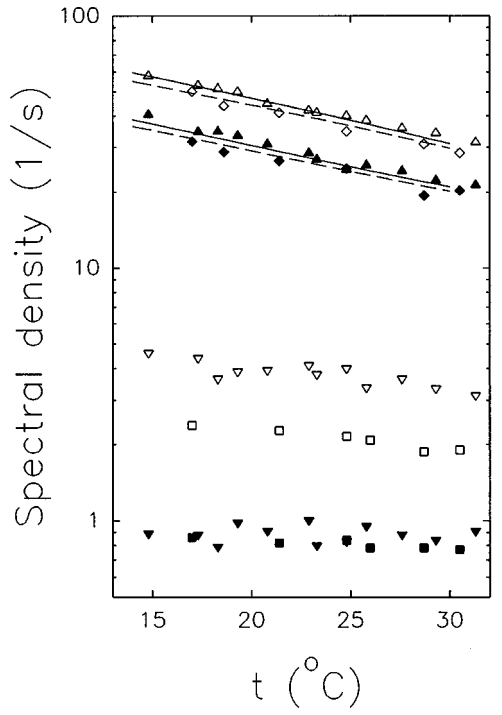

FIG. 4. Experimental (symbols) and fitted (lines) spectral densities of C_0, and experimental spectral density for C_5 in 5CB-d_{15}. The open symbols denote $J_1(\omega_0)$, while the closed symbols denote $J_2(2\omega_0)$. The upward triangles represent the C_0 data at 15.3 MHz, while the diamonds represent its data at 46 MHz. The downward triangles represent the C_5 data at 15.3 MHz, while the squares represent its data at 46 MHz. Solid and long dashed lines denote fitted spectral densities for C_0 at 15.3 and 46 MHz, respectively. The experimental data were reproduced from Ref. [11].

where the sum k is over the five different temperatures, and $m = 0$, 1, or 2 except for the ring deuterons, $m = 1$ or 2. The fitting quality Q is given by the percentage mean squared deviation,

$$Q=\frac{F\times 100}{\sum_k \sum_{\omega_0} \sum_i \sum_m [J_m^{(i)\mathrm{expt}}(m\omega_0)]_k^2}\%. \tag{18}$$

Minimizing F tends to emphasize spectral densities of larger values [i.e., $J_0^{(i)}(0)$] and to make the fits to J_1 and J_2 progressively worse for deuterons near the end of the chain. Since this study focuses on the T_2 data, the bias towards J_0 is perhaps justified. Over the narrow temperature range studied here, we found that the temperature behaviors of diffusion constants and jump constant k_3 can be assumed to follow simple Arrhenius-type relations, giving

$$D_x=D_x^0\exp(-E_a^{D_x}/RT), \tag{19}$$

$$D_z=D_z^0\exp(-E_a^{D_z}/RT), \tag{20}$$

$$D_R=D_R^0\exp(-E_a^{D_R}/RT), \tag{21}$$

$$k_3=k_3^0\exp(-E_a^{k_3}/RT), \tag{22}$$

where the pre-exponentials D_x^0, D_z^0, D_R^0, and k_3^0, and their corresponding activation energies $E_a^{D_x}$, $E_a^{D_z}$, $E_a^{D_R}$, and $E_a^{k_3}$ are global parameters. When such a relation cannot be assumed for a target parameter like k_1, k_2 and the prefactor A, it is still possible to introduce an interpolating relation linking its values at various temperatures. As k_1, k_2, and A are weakly temperature dependent, we model them by linear relations

$$k_1=k_1'-k_1''(T-T_{\min}), \tag{23}$$

$$k_2=k_2'+k_2''(T-T_{\min}), \tag{24}$$

$$A=A'-A''(T-T_{\min}), \tag{25}$$

where the temperature $T_{\min}$ is the lowest temperature used in our global analysis, and k_1', k_1'', k_2', k_2'', A', and A'' are global parameters. Therefore, Eqs. (19)–(25) allow us to find all the target parameters at different temperatures. Now the 14 global parameters are optimized by fitting a total of 120 spectral densities (from 5 temperatures) for a given ω_c value. For convenience, the diffusion and jump rate preexponentials are not used as global parameters. Rather Eqs. (19)–(22) are rewritten in terms of the activation energies and the diffusion and jump constants D_x',D_z',D_R',k_3' at 287.3 K ($T_{\min}$). Together with k_1,k_2, and A at 287.3 K, and temperature coefficients k_1'', k_2'', and A'' form the set of global parameters used in our minimization. Initial model parameters at the $T_{\min}$ were first obtained by an individual target analysis.

We assume for simplicity that ω_c is constant in the nematic phase of 5CB. The assumption is probably good because of the narrow temperature range studied here. Several high cutoff frequency values, between 1 and 20 MHz, were tested; the Q values continued to improve as the value of high cutoff frequency was reduced to 1 MHz. In these tests, director fluctuations and the cross term were considered in J_1 and/or J_2 unless $\omega_c/2\pi$ was less than a few MHz. It is indeed difficult in this study to choose a proper value for the high

TABLE I. Motional parameters derived from a global analysis of spectral densities using $\omega_c/2\pi = 1$ MHz and $\omega_1/2\pi = 98$ Hz. k_2 was found to be nearly constant ($=6.99\times10^{14}$ s^{-1}) at these temperatures.

T (K)	k_1 (10^{10} s^{-1})	k_3 (10^{12} s^{-1})	D_x (10^7 s^{-1})	D_z (10^9 s^{-1})	D_R (10^9 s^{-1})	A (10^{-5} s$^{1/2}$)
303.3	0.96	9.29	6.29	1.50	1.48	2.45
299.3	4.49	7.06	5.16	1.20	1.38	2.40
295.3	8.02	5.32	4.22	0.95	1.29	2.44
291.3	11.55	3.98	3.42	0.75	1.20	2.52
287.3	15.08	2.95	2.76	0.58	1.12	2.59 ± 0.23

TABLE II. Calculated spectral densities (in s^{-1}) for C_1-C_4 deuterons due to director fluctuations and molecular reorientation at 295.3 K.

C_i	$J_{0R}(0)$	$J_{0DF}(0)$	$J_0^{expt}(\omega)$
C_1	32.8	78.0	130.3
C_2	17.0	37.7	62.2
C_3	16.0	42.9	53.5
C_4	6.7	19.7	31.5

cutoff frequency. However, in a similar study of MBBA [28] the high cutoff frequency was estimated to be 10 MHz (or lower) with a Q factor of about 1%. We note also that a recent proton NMR study [33] of 5CB has suggested that the high cutoff frequency is of the order of 1 kHz. We think that 5CB has a small high cutoff frequency like MBBA, but not as low as 1 kHz as suggested. Hence, we have assumed that $\omega_c/2\pi = 1$ MHz in the following discussion. In addition, the low cutoff frequency $\omega_1/2\pi$ has been estimated to be 98 Hz using $\omega_1 = K/\eta\xi^2$. The fitting quality Q factor was found to be 1.8% in the present study. Our results show that $E_a^{D_x}$ (37.3 ± 1.3 kJ/mol) is a little smaller than $E_a^{D_z}$ (42.6$\pm$1.9 kJ/mol), and $E_a^{D_R}$ is equal to 12.7$\pm$1.8 kJ/mol. Now $E_a^{D_x} < E_a^{D_z}$ was found when only the T_1 data were analyzed [11] using the numerical solutions given in Ref. [34] and their Eqs. (20) and (21). This previous T_1 analysis had a problem, since the mentioned equations of Ref. [34] contained errors as pointed out by us [24,30]. The present study has avoided this by directly solving the rotational diffusion equation. The error limit for a particular global parameter was estimated by varying the one under consideration while keeping all other global parameters identical to those for the minimum F, to give an approximate doubling in the F value. The activation energy for the three-bond (k_3) motion is 51.9 kJ/mol. The model parameters (3 k's, 3 D's, and A) for $\omega_c/2\pi = 1$ MHz at each chosen temperature are summarized in Table I. The activation energies and the preexponentials ($k_3^0 = 8.07\times10^{21}$ s^{-1}, $D_x^0 = 1.68\times10^{14}$ s^{-1}, $D_z^0 = 3.25\times10^{16}$ s^{-1}, and $D_R^0 = 3.29\times10^{11}$ s^{-1}) are used to plot the fitted spectral density curves in Figs. 2–4. The observed frequency dependences in $J_1^{(i)}(\omega)$ and $J_2^{(i)}(2\omega)$ are due to ''slow'' molecular rotations. The fits between the experimental and calculated spectral densities are acceptable, in particular for $J_0^{(i)}(0)$. The calculated contributions to $J_0^{(i)}(0)$, as a result of the fitting procedure, from director fluctuations and molecular motions are summarized for $T = 295.3$ K in Table II. It is clear from this table that without director fluctuations, the calculated $J_0^{(i)}(0)$ would be too small even allowing for large uncertainties in $J_0^{(i)expt}(0)$. As seen in Figs. 2 and 3, there are some systematic deviations between the experimental and fitted spectral densities, especially $J_1^{(i)}(\omega)$ and $J_2^{(i)}(2\omega)$ at 46 MHz for $i = 3$ or 4. Using typical values [35] of $K = 6.8\times10^{-12}$ N and $\eta = 6.3\times10^{-2}$ Pa s, $A = 1\times10^{-5}$ $s^{1/2}$ is calculated from Eq. (4) at 300 K. Thus, the derived A (Table I) values appear to be close to the theoretical value. It is noted that A is almost independent of the temperature and its error bar is indicated in Table I. The error bar for D_x^0 is given by $(1.1-3.0)\times10^{14}$ s^{-1}, while that of D_z^0 is $(1.53-7.0)\times10^{16}$ s^{-1}. Similarly, D_R^0 varies from 1.1×10^{11} s^{-1} to 4.85×10^{11} s^{-1}, and k_3^0 varies from 1.35×10^{21} s^{-1} to 1.0×10^{24} s^{-1} (25% increase in F) and $E_a^{k_3}$ varies between 56.2 and 40.5 kJ/mol (25% increase in F). Now k_2 is found to be nearly constant and equal to 6.99×10^{14} s^{-1}. The fits are very insensitive to higher k_2 values and its lower error limit is 3.0×10^{11} s^{-1}. The error bar for k_1' is given between 1.13×10^{11} s^{-1} and 9.5×10^{11} s^{-1} (50% increase in F). The error limits specified for 25 or 50% increase in F were necessary because of their insensitivity in the fits. It is interesting to compare the above results with those obtained in MBBA. At the same reduced temperature ($T/T_c = 0.96$), A of MBBA is about 30% smaller than that of 5CB. While D_x is similar for the two nematogens, the spinning motion of MBBA is faster by a factor of 2. The slower spinning motion of 5CB could be due to the large terminal dipole in the 5CB molecule. When comparing their internal dynamics, k_1 and k_3 are more or less comparable in values at this reduced temperature, but the k_2 rate for 5CB appears to be four orders of magnitude higher. A plausible explanation is the difference in their chain lengths.

In conclusion, we have demonstrated in the present study how a standard high field spectrometer can be used to study director fluctuations in the nematic phase of 5CB by means of deuteron T_2 measurements. This is inferred from the fact that $J_0^{(i)expt}(0)$ for the methylene deuterons cannot be accounted for by the molecular rotation and internal motions in the flexible chain. A possible and probable explanation is to invoke director fluctuations. The ability to study the second-order contribution from director fluctuations in 5CB is attributed to its high cutoff frequency being small. Incidentally both 5CB and MBBA, in which we have detected second-order director fluctuations, are room temperature nematogens.

ACKNOWLEDGMENTS

The financial support of the Natural Sciences and Engineering Council of Canada and Brandon University is gratefully acknowledged. We thank Mr. N. Finlay for technical support and Professor C. Zannoni for making his program in Ref. [29] available to us.

[1] P. Pincusm, Solid State Commun. **7**, 415 (1969).

[2] R. Y. Dong, *Nuclear Magnetic Resonance of Liquid Crystals,* 2nd ed. (Springer-Verlag, New York, 1997).

[3] *Nuclear Magnetic Resonance of Liquid Crystals,* edited by J. W. Emsley (Reidel, Dordrecht, 1985); C. G. Wade, Annu. Rev. Phys. **28**, 47 (1977).

[4] R. R. Vold and R. L. Vold, *The Molecular Dynamics of Liquid Crystals,* edited by G. R. Luckhurst and C. A. Veracini

(Kluwer Academic, Dordrecht, 1994).
[5] R. Y. Dong, J. Lewis, E. Tomchuk, and E. Bock, J. Chem. Phys. **69**, 5314 (1978).
[6] R. Y. Dong and X. Shen, Phys. Rev. E **49**, 538 (1994).
[7] T. M. Barbara, R. R. Vold, R. L. Vold, and M. E. Neubert, J. Chem. Phys. **82**, 1612 (1985).
[8] F. Noack, Progr. NMR Spectrosc. **18**, 171 (1986); K. H. Schweikert and F. Noack, Mol. Cryst. Liq. Cryst. Sci. Technol., Sect. A **212**, 33 (1992).
[9] R. Y. Dong, Chem. Phys. Lett. **251**, 387 (1996).
[10] P. A. Beckmann, J. W. Emsley, G. R. Luckhurst, and D. L. Turner, Mol. Phys. **59**, 97 (1986).
[11] R. Y. Dong and G. M. Richards, Mol. Cryst. Liq. Cryst. Sci. Technol., Sect. A **262**, 339 (1995).
[12] A. Ferrarini, G. J. Moro, and P. L. Nordio, Liq. Cryst. **8**, 593 (1990).
[13] J. S. Lewis, E. Tomchuk, H. M. Hutton, and E. Bock, J. Chem. Phys. **78**, 632 (1983).
[14] J. W. Doane, C. E. Tarr, and M. A. Nickerson, Phys. Rev. Lett. **33**, 620 (1974).
[15] T. E. Faber, Proc. R. Soc. London, Ser. A **353**, 277 (1977).
[16] R. L. Vold, R. R. Vold, and M. Warner, J. Chem. Soc., Faraday Trans. **84**, 997 (1988).
[17] G. van der Zwan and L. Plomp, Liq. Cryst. **4**, 133 (1989).
[18] E. A. Joghems and G. van der Zwan, J. Phys. II **6**, 845 (1996).
[19] J. H. Freed, J. Chem. Phys. **66**, 4183 (1977).
[20] P. Ukleja, J. Pirs, and J. W. Doane, Phys. Rev. A **14**, 414 (1976).
[21] P. L. Nordio and P. Busolin, J. Chem. Phys. **55**, 5485 (1971); P. L. Nordio, G. Rigatti, and U. Segre, *ibid.* **56**, 2117 (1972).
[22] R. Y. Dong, Phys. Rev. A **43**, 4310 (1991).
[23] A. Arcioni, R. Tarroni, and G. Zannoni, Nuovo Cimento D **10**, 1409 (1989); Liq. Cryst. **6**, 63 (1989).
[24] R. Y. Dong, Mol. Phys. **88**, 979 (1996).
[25] H. Y. Carr and E. M. Purcell, Phys. Rev. **94** , 630 (1954).
[26] S. B. Ahmad, K. J. Packer, and J. M. Ramsden, Mol. Phys. **33**, 857 (1977).
[27] M. Warner, Mol. Phys. **52**, 677 (1984).
[28] R. Y. Dong and X. Shen, J. Phys. Chem. **101**, 4673 (1997).
[29] R. Tarroni and C. Zannoni, J. Chem. Phys. **95**, 4550 (1991).
[30] R. Y. Dong and X. Shen, J. Chem. Phys. **105**, 2106 (1996).
[31] A. Ferrarini, G. J. Moro, and P. L. Nordio, Liq. Cryst. **8**, 593 (1990).
[32] W. H. Press, B. P. Flannery, S. A. Teukolsky, and W. T. Vetterling, *Numerical Recipes* (Cambridge University Press, Cambridge, UK, 1986).
[33] F. Grinberg and R. Kimmich, J. Chem. Phys. **103**, 365 (1995).
[34] R. R. Vold and R. L. Vold, J. Chem. Phys. **88**, 1443 (1988).
[35] G. Vertogen and W. H. de Jeu, *Thermotropic Liquid Crystals* (Springer-Verlag, Berlin, 1988); *Introduction to Liquid Crystals*, edited by E. B. Priestley, P. J. Wojtowicz, and P. Sheng (Plenum Press, New York, 1974).